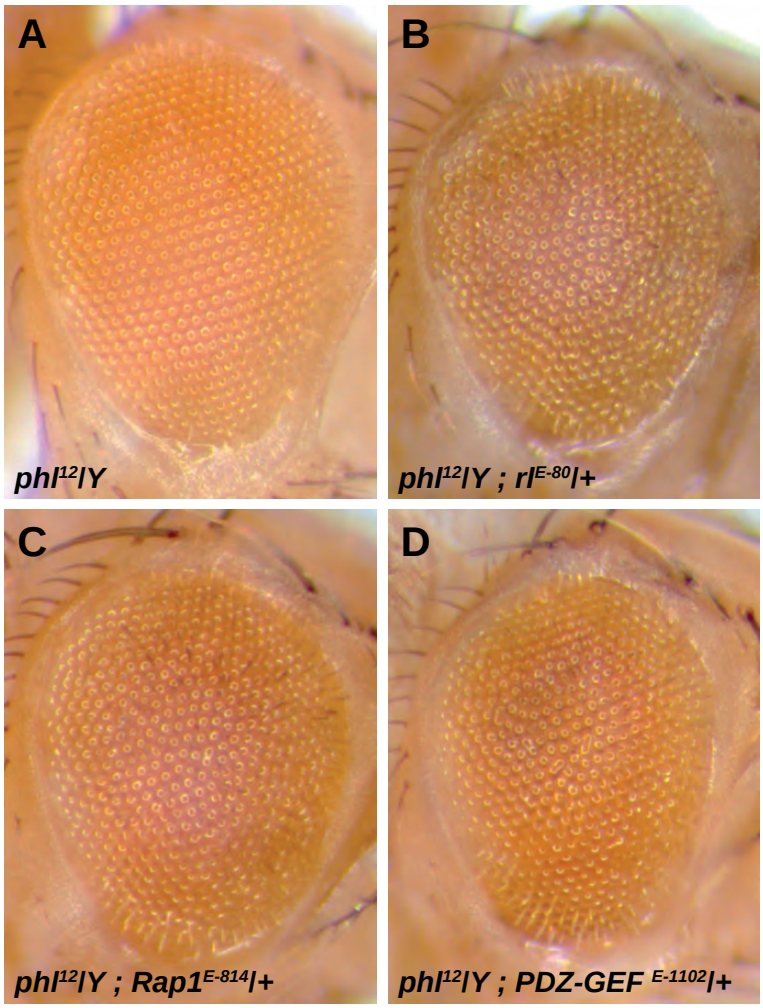

Figure S1 *Rap1* and *PDZ-GEF* alleles genetically interact with a hypomorphic allele of *raf* (*phl*^{12}). (A-D) Micrographs of adult eyes of the indicated genotypes. A *rolled* (*rl*) loss-of-function allele (B) was used as reference for enhanced eye roughness. Anterior is to the right.

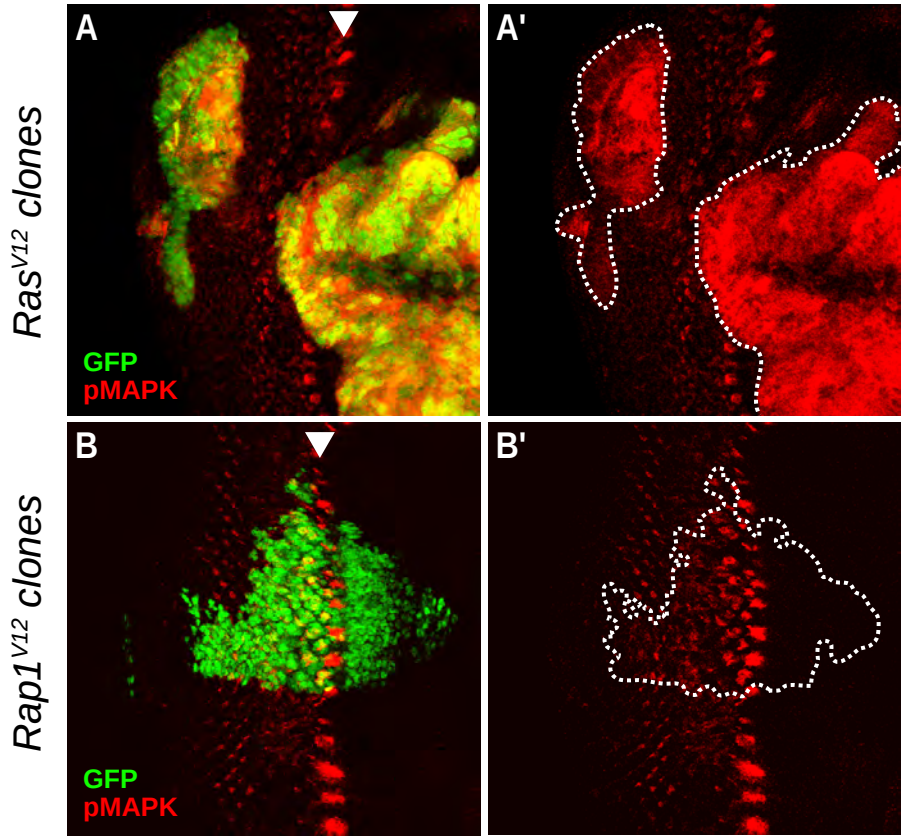

Figure S2 Unlike *Ras^{V12}*, clonal overexpression of *Rap1^{V12}* during eye development does not promote ectopic activation of MAPK (pMAPK). (A-A') *UAS-Ras^{V12}* and (B-B') *UAS-Rap1^{V12}* were clonally expressed in third instar eye discs and visuallized using the FLP-out / Gal4 system (GFP-positive cells). The arrowhead marks the position of the morphogenetic furrow. Anterior is to the right.

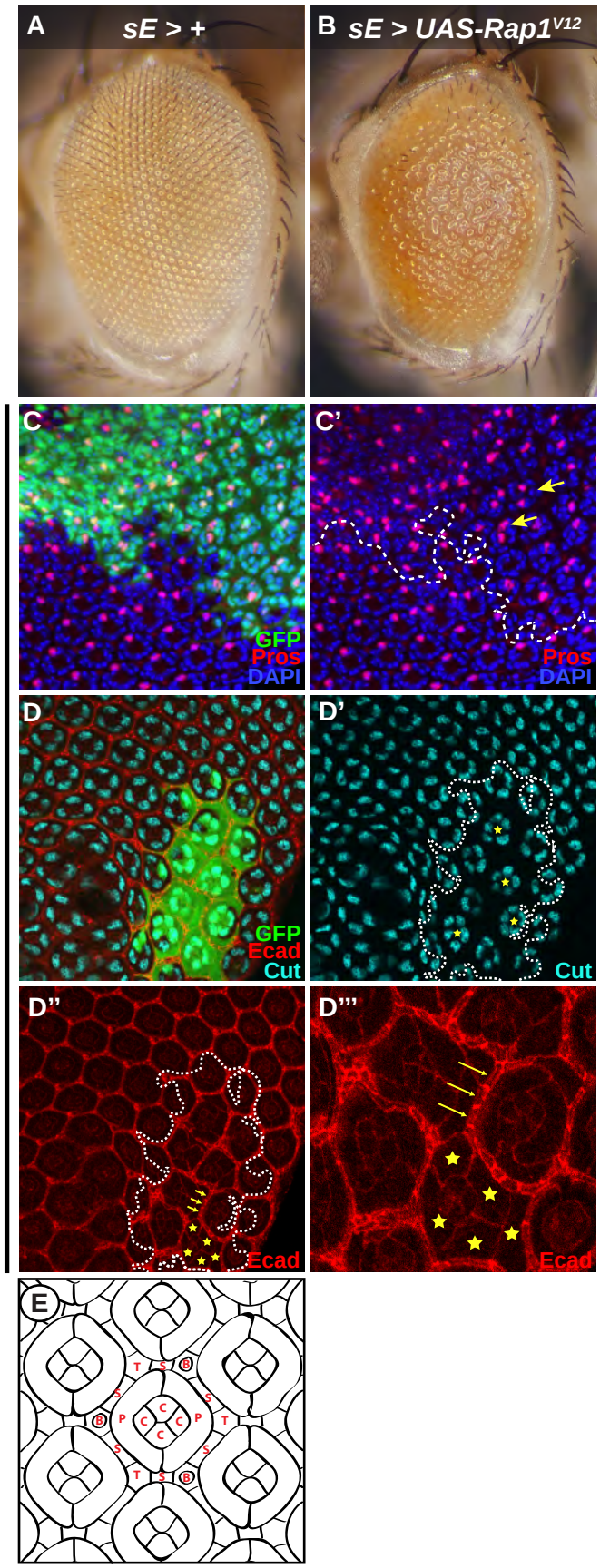

Figure S3 Rap1^{V12} is constitutively active. Adult retina expressing (A) *sE-Gal4* alone or (B) *sE-Gal4* combined with *UAS-Rap1^{V12}*. (C-D''') Random clones (GFP-positive cells) expressing Rap1^{V12} in pupal eye discs (45h after pupal formation) were induced by heat shock using the FLP-out/Gal4 system. Pupal eye discs were then immunostained with (C-C'') anti-Prospero to reveal R7 (Pros-positive) cells (nuclei outlined by DAPI) or (D-D''') anti-Ecad and anti-Cut to reveal cell outlines and cone cells, respectively. Dotted lines (C'-D'') mark the Rap1^{V12}-expressing clonal areas. (C') Arrows point to examples of ommatidia containing extra R7 cells. Rap1^{V12} expression also leads to extra cone cells (examples of five cone cells instead of the normal four cone cells per ommatidium are marked by a star in D'), and extra primary and secondary pigment cells (stars and arrows, respectively, in D''). (D''') Enlarged area encompassing the ommatidia where extra primary and secondary pigment cells are respectively highlighted by stars and arrows in D''. (E) Schematic representation of the apical cell outlines of a 45h pupal eye disc. Typically, at an apical focal plane, cell outlines reveal the two primary (P), six secondary (S), and three tertiary (T) pigment cells as well as the three mechano-sensory bristle (B) cells and the four cone (C) cells composing a normal ommatidium (Wolff and Ready, 1991).

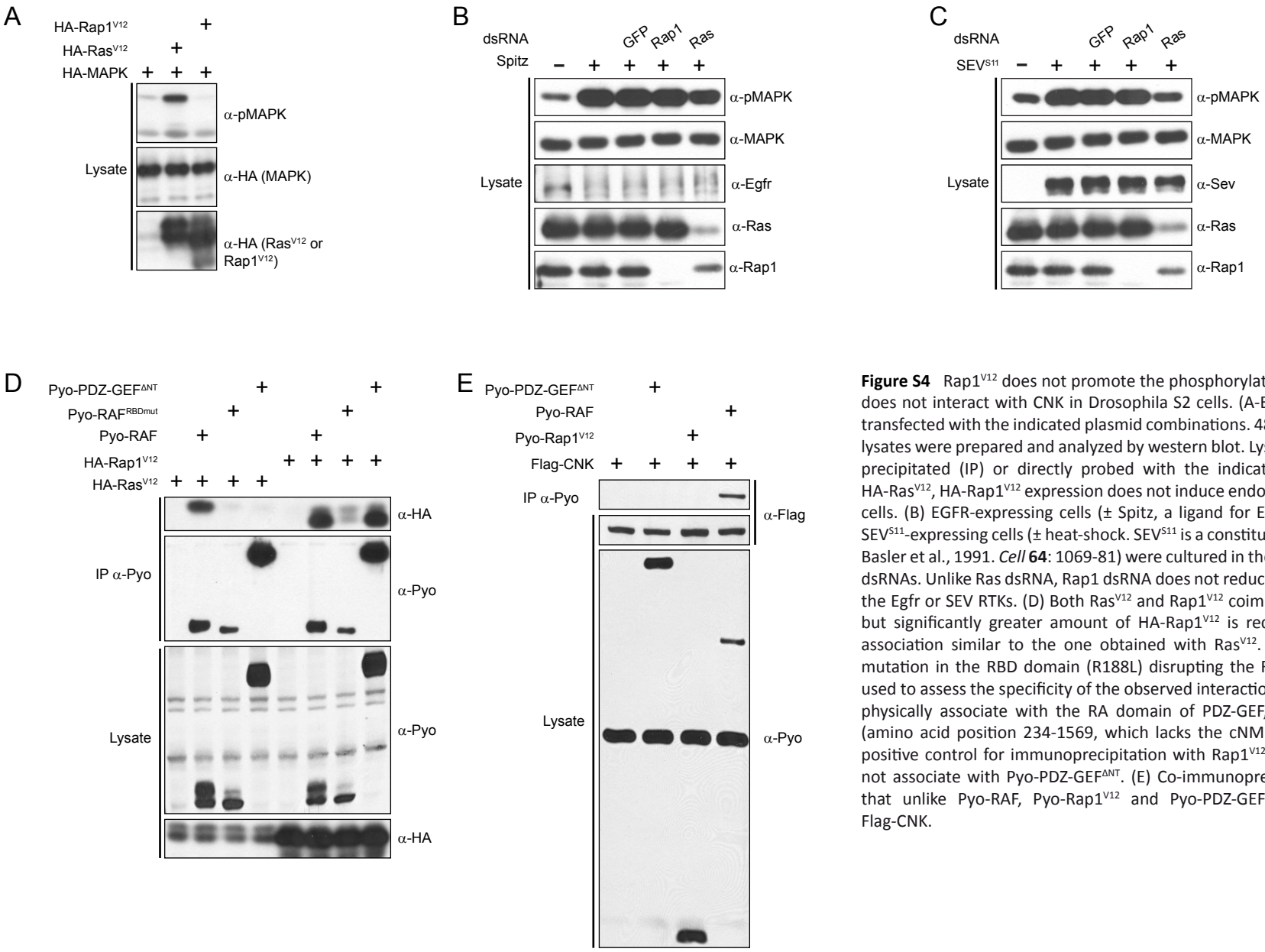

Figure S4 Rap1^{V12} does not promote the phosphorylation of MAPK (pMAPK) and does not interact with CNK in Drosophila S2 cells. (A-E) S2 cells were transiently transfected with the indicated plasmid combinations. 48 hrs post-transfection, cell lysates were prepared and analyzed by western blot. Lysates were either immunoprecipitated (IP) or directly probed with the indicated antibodies. (A) Unlike HA-Ras^{V12}, HA-Rap1^{V12} expression does not induce endogenous pMAPK levels in S2 cells. (B) EGFR-expressing cells (± Spitz, a ligand for EGFR) or (C) heat-inducible SEV^{S11}-expressing cells (± heat-shock. SEV^{S11} is a constitutively active variant of SEV; Basler et al., 1991. *Cell* **64**: 1069-81) were cultured in the presence of the indicated dsRNAs. Unlike Ras dsRNA, Rap1 dsRNA does not reduce pMAPK levels induced by the Egfr or SEV RTKs. (D) Both Ras^{V12} and Rap1^{V12} coimmunoprecipitate with RAF, but significantly greater amount of HA-Rap1^{V12} is required to reach a level of association similar to the one obtained with Ras^{V12}. RAF^{RBDmut} harbors a point mutation in the RBD domain (R188L) disrupting the Ras-RAF association and is used to assess the specificity of the observed interactions. Since Rap1 is known to physically associate with the RA domain of PDZ-GEF, we used Pyo-PDZ-GEF$^{\Delta NT}$ (amino acid position 234-1569, which lacks the cNMP domain; Figure 2F) as a positive control for immunoprecipitation with Rap1^{V12}. Interestingly, Ras^{V12} does not associate with Pyo-PDZ-GEF$^{\Delta NT}$. (E) Co-immunoprecipitation assays revealed that unlike Pyo-RAF, Pyo-Rap1^{V12} and Pyo-PDZ-GEF$^{\Delta NT}$ fail to associate with Flag-CNK.

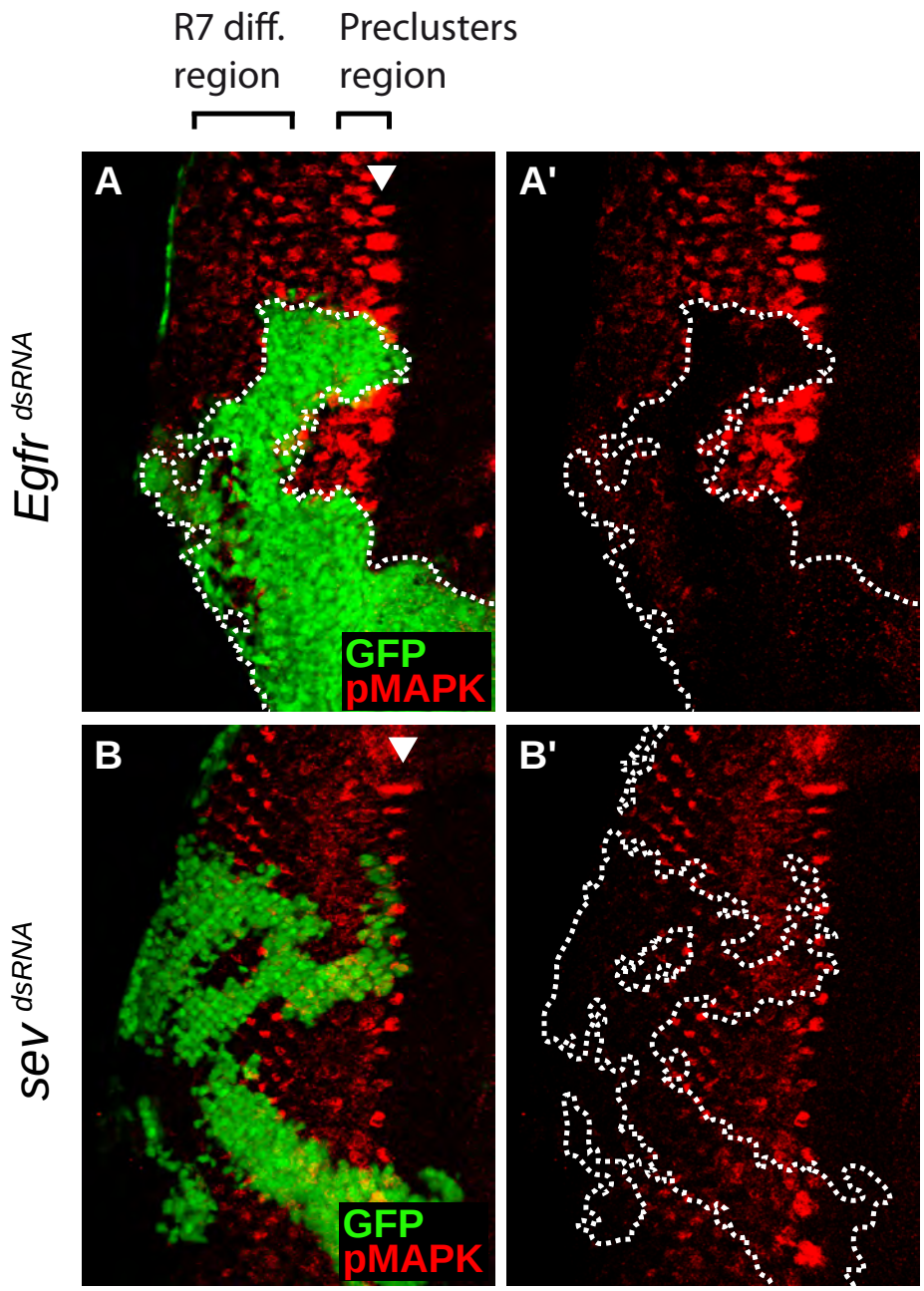

Figure S5 Comparison of the eye disc areas controlled by EGFR and SEV leading to MAPK activation. (A-A' and B-B') Random clones (GFP positive cells) expressing the indicated dsRNAs were induced using the FLP-out Gal4 system and phosphorylated MAPK (pMAPK) was monitored by immunofluorescence in third instar larval eye discs. Arrowheads refer to the position of the morphogenetic furrow. Anterior is to the right.

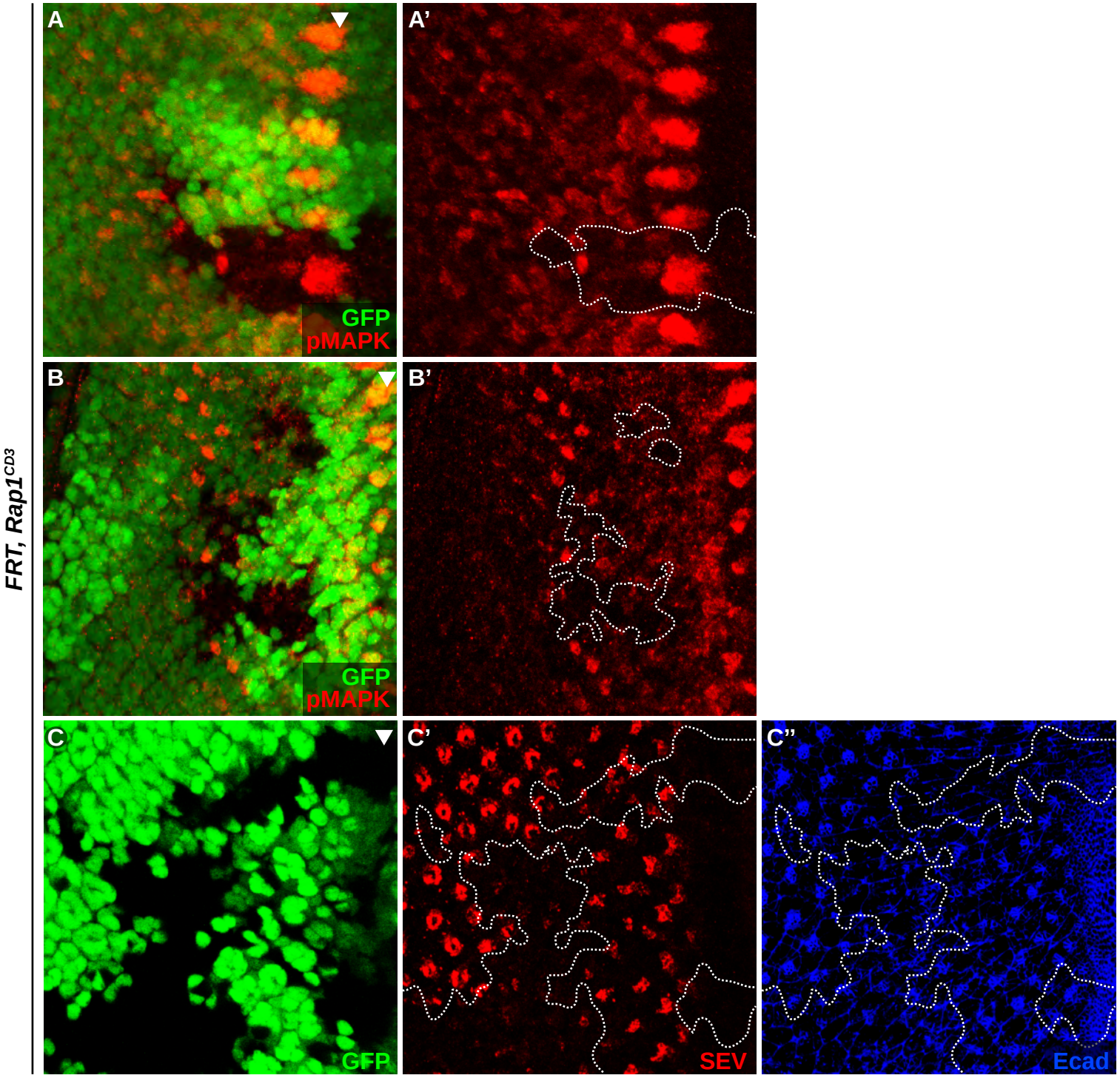

Figure S6 Clonal analysis of *Rap1*^{CD3} null allele confirms results obtained with *Rap1* dsRNA in third instar eye discs. (A-A' to C-C'') Random homozygous clones (GFP-negative cells) for the *Rap*^{CD3} allele in third instar eye discs were induced using the FLP/FRT system. Eye discs were then immunostained with (A' and B') anti-pMAPK, (C') anti-SEV and (C'') anti-Ecad antibodies. Loss of Rap1 activity does not impede pMAPK levels in cells close to the morphogenetic furrow (A'), but significantly reduces pMAPK levels in posterior areas (B') corresponding to the R7 differentiation region, wherein SEV activity is required. Arrowheads mark the position of the morphogenetic furrow. Anterior is to the right.

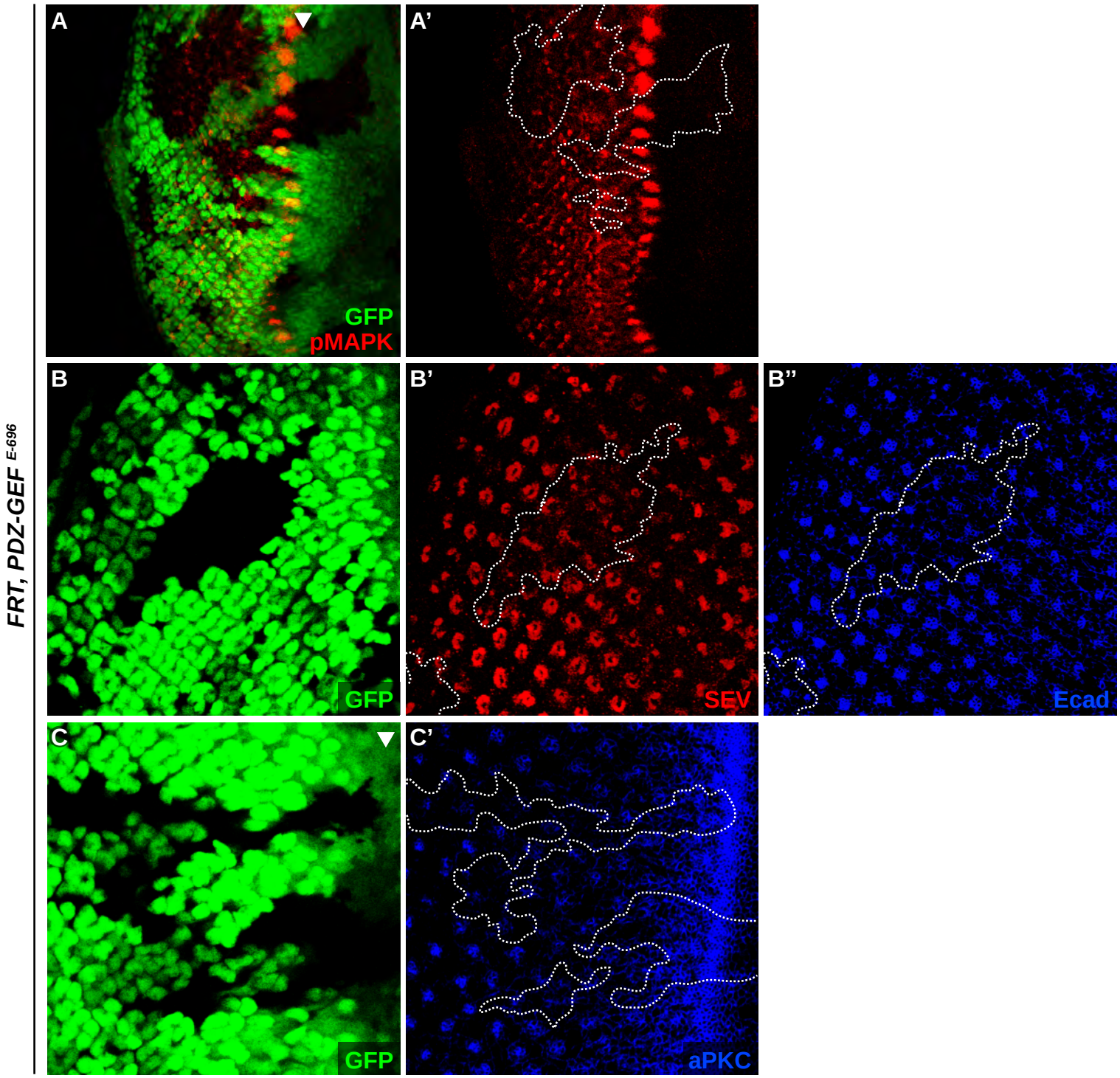

Figure S7 Clonal analysis of *PDZ-GEF*$^{E\text{-}696}$ null allele confirms results obtained with *PDZ-GEF* dsRNA in third instar eye discs. (A-A' to C-C'') Random homozygous clones (GFP-negative cells) for the *PDZ-GEF*$^{E\text{-}696}$ allele in third instar eye discs were induced using the FLP/FRT system. Eye discs were then immunostained with (A') anti-pMAPK, (B') anti-SEV, (B'') anti-Ecad, and (C') anti-aPKC antibodies. Loss of PDZ-GEF activity does not impede pMAPK levels in cells close to the morphogenetic furrow (A'), but reduces pMAPK levels in posterior areas corresponding to the R7 differentiation region, wherein SEV activity is required. Arrowheads mark the position of the morphogenetic furrow. Anterior is to the right.

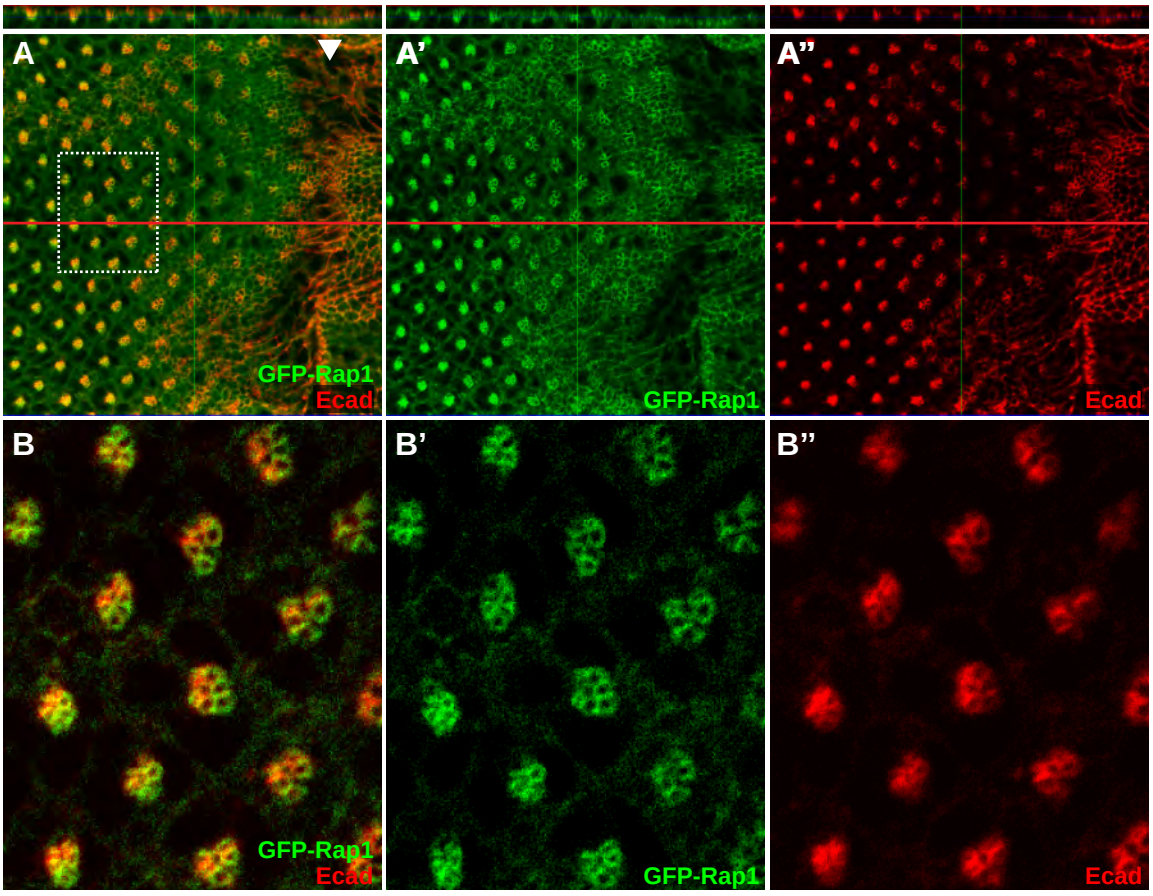

Figure S8 Expression pattern and apical subcellular localization in third instar eye disc of *GFP-Rap1* under the endogenous *Rap1* promoter. (A-A'') GFP-Rap1 accumulates at adherens junctions of developing ommatidia as revealed by co-localization with E-cadherin (Ecad) staining. The red line across each panel corresponds to the position of the optical cross-section shown at the top. (B-B'') Higher magnification of the boxed area shown in (A). Arrowheads denote the position of the morphogenetic furrow. Anterior is to the right.

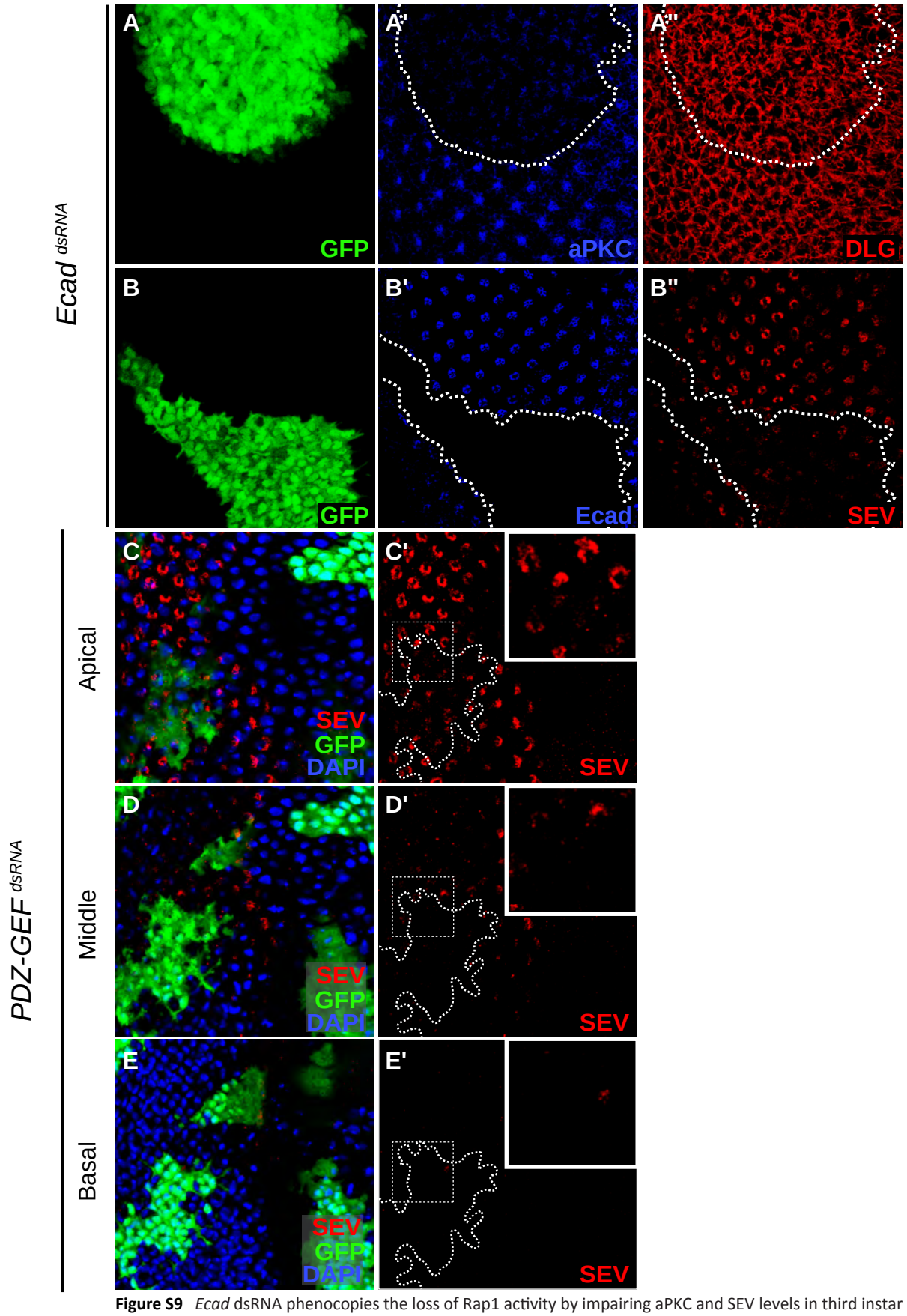

Figure S9 *Ecad* dsRNA phenocopies the loss of Rap1 activity by impairing aPKC and SEV levels in third instar eye discs. (A-A'' to E-E') Random clones (GFP-positive cells) expressing the indicated dsRNAs in third instar larval eye discs were induced using the FLP-out / Gal4 system. Eye discs were then immunostained with (A') anti-aPKC, (A'') anti-DLG, (B') anti-Ecad, and (B'', C'-E') anti-SEV antibodies. The loss of Rap1 signaling, as examplified by depleting PDZ-GEF levels (C-E), reduces SEV levels that normally populate the apical domain and does not lead to a relocalization of SEV to basolateral membranes. The boxed areas in (C'-E') are shown enlarged at the top right corner of each panel. Anterior is to the right.

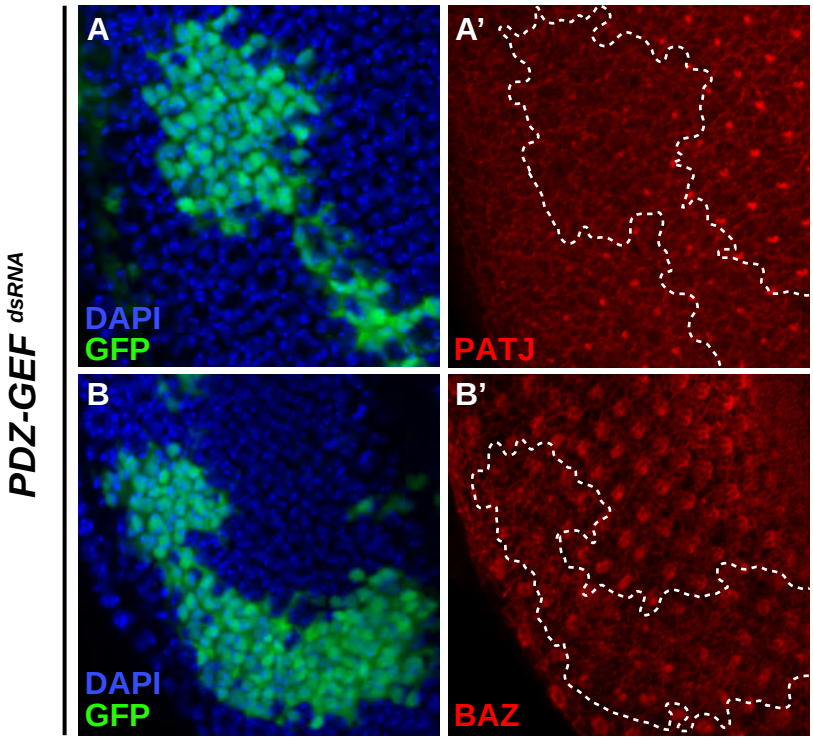

Figure S10 Knockdown of PDZ-GEF during eye development impairs apical localization of PATJ and Bazooka. Random clones (GFP-positive cells) expressing *PDZ-GEF* dsRNA were induced using the FLP-out / Gal4 system. Eye discs were then immunostained with (A') anti-PATJ or (B') anti-Bazooka. Anterior is to the right.

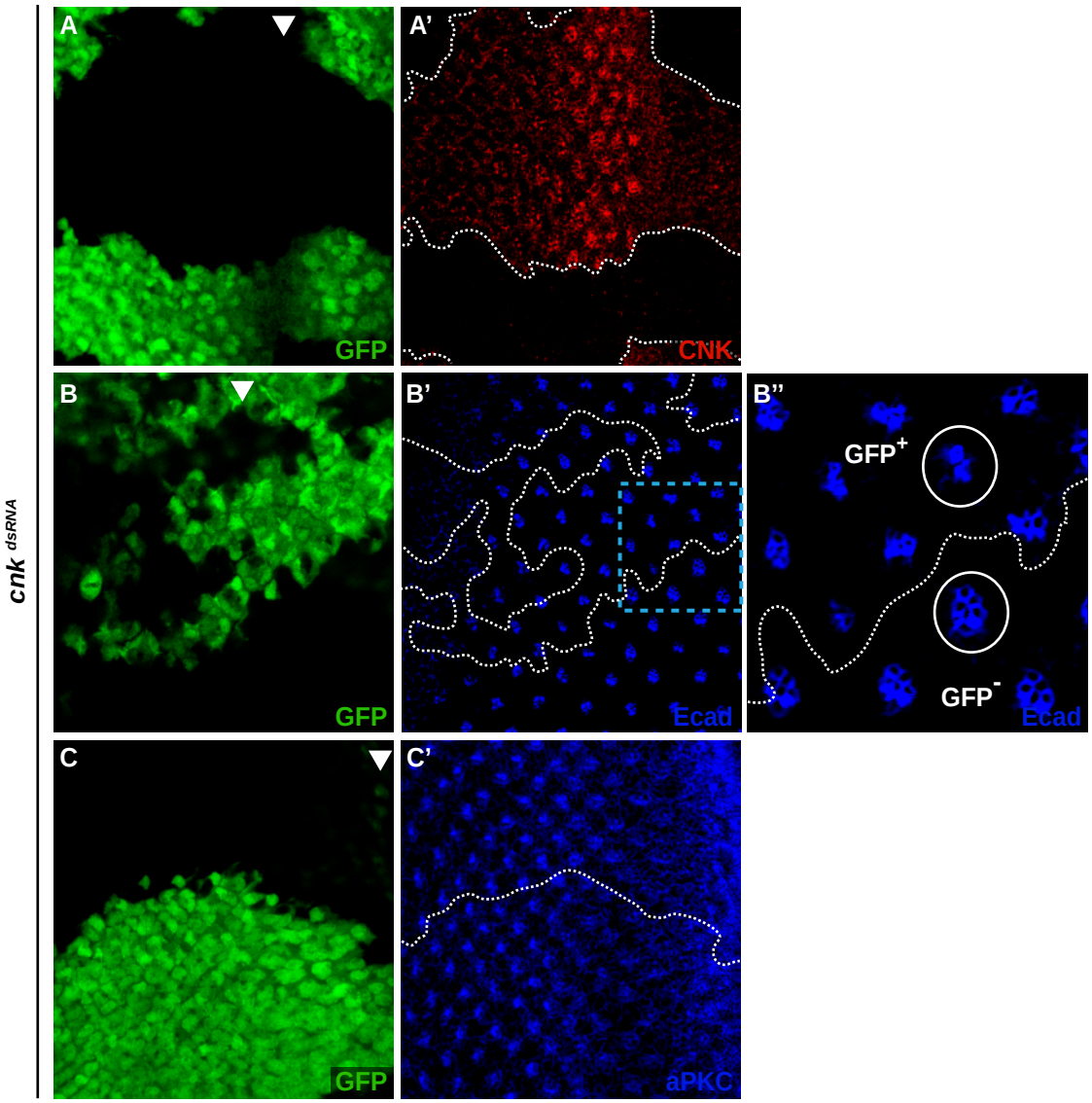

Figure S11 Knockdown of CNK in third instar larval eye discs has no impact on the level of adherens junction or apical domain markers per individual ommatidial cell. (A-A' to C-C') Random clones (GFP-positive cells) expressing *cnk* dsRNA in third instar eye discs were induced using the FLP-out / Gal4 system. Eye discs were then immunostained with (A') anti-CNK, (B' and B'') anti-Ecad; or (C') anti-aPKC antibodies. B'' corresponds to the boxed area shown in B'. Because CNK depletion impedes cell differentiation, less cells join ommatidial clusters and as a result reduces the overall area that normally stains positive for Ecad in each ommatidium. Circles in B'' highlight typical examples of the size difference between ommatidial clusters expressing (GFP+) or not (GFP–) *cnk* dsRNAs. However, Ecad or aPKC levels per cell in differentiating *cnk* dsRNA-expressing cells do not appear to be reduced compared to control cells. Arrowheads denote the position of the morphogenetic furrow. Anterior is to the right.

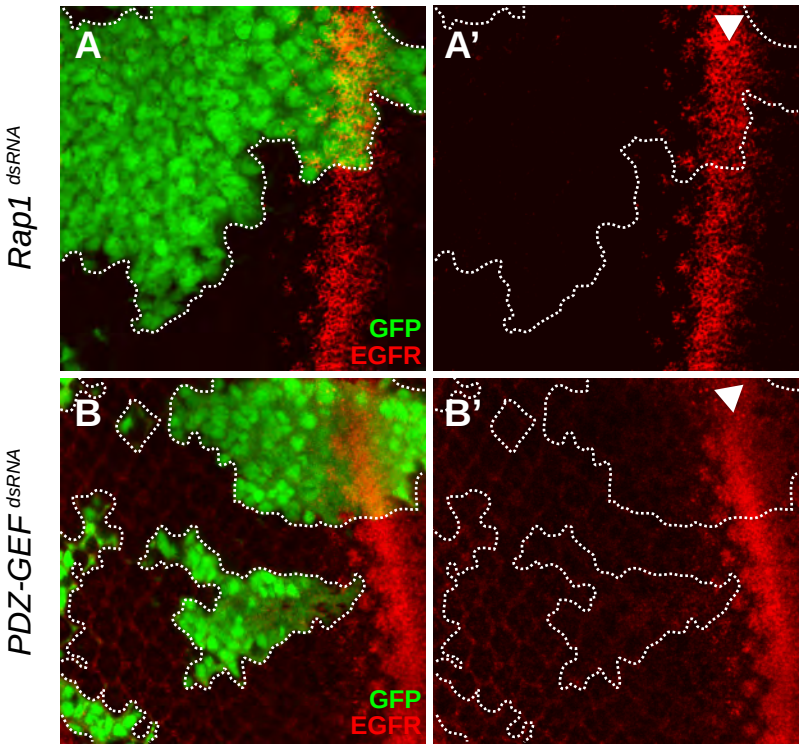

Figure S12 Reduction of Rap1 activity during eye development does not alter Egfr expression pattern. (A-A') Rap1 dsRNA or (B-B') PDZ-GEF dsRNA were clonally expressed (marked by GFP) in the third instar eye discs using the FLP-out Gal4 system. Discs were then stained with an anti-Egfr antibody. The arrowhead refers to the position of the morphogenetic furrow. Anterior is to the right.

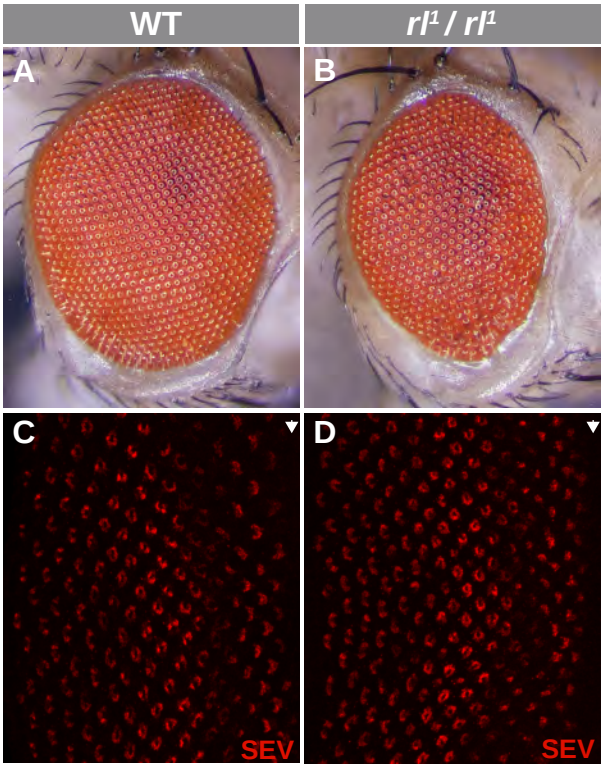

Figure S13 Reduction of MAPK activity does not alter SEV levels. Adult fly retinae (A-B) or third instar eye discs stained using an anti-SEV antibody (C-D) are shown. Compared to WT (A-C), the homozygous *rolled*^{1} (*rl*^{1}) mutation (B-D) causes eye roughness owing to the loss ommatidial cells, but does not modify SEV levels or expression pattern. Arrowheads mark the position of the morphogenetic furrow. Anterior is to the right.

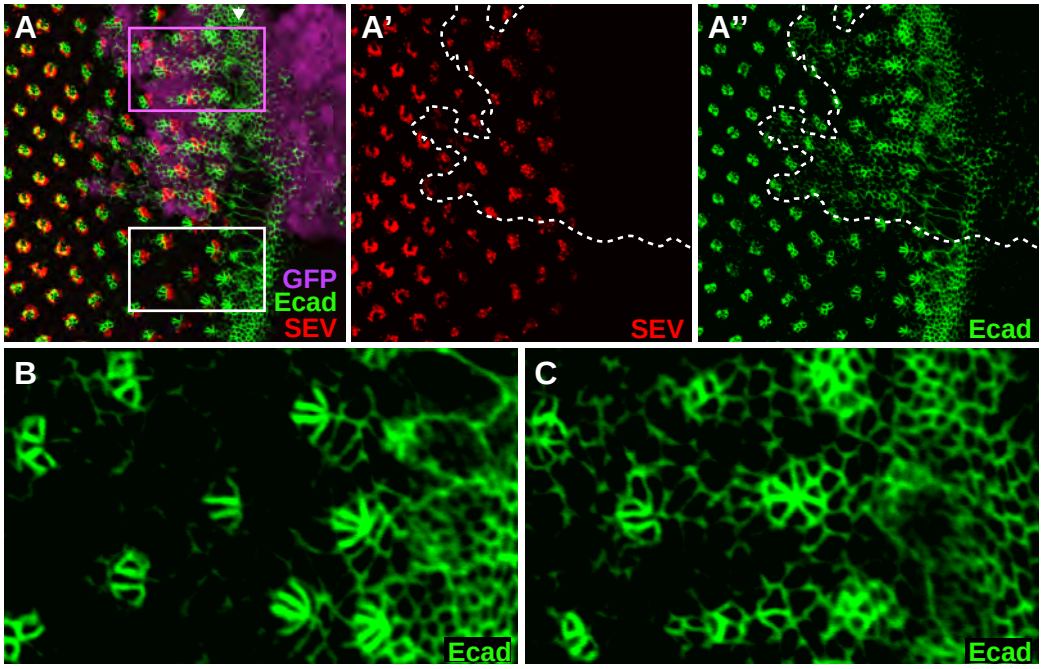

Figure S14 Rap1^{V12} does not alter SEV expression, but perturbs ommatidial cluster assembly. (A-A'') Random clones (GFP-positive cells) expressing Rap1^{V12} in third instar eye discs were induced by heat shock using the FLP-out/Gal4 system. Tissues were then immunostained with anti-SEV and anti-Ecad antibodies. Dotted line in (A'-A'') marks the Rap1^{V12}-expressing clonal area. The white and magenta boxes in (A) encompass control and Rap1^{V12}-expressing areas that are respectively shown enlarged in (B) and (C). Arrowheads denote the position of the morphogenetic furrow. Anterior is to the right.